

Supporting Information

Role of O–H···O/S conventional hydrogen bonds in considerable C_{sp2}–H blue-shift in the binary systems of acetaldehyde and thioacetaldehyde with the substituted carboxylic and thiocarboxylic acids

Nguyen Truong An¹, Nguyen Thi Duong¹, Nguyen Ngoc Tri,^{1,2} Nguyen Tien Trung^{1,2*}

¹Faculty of Natural Sciences, Quy Nhon University, Quy Nhon, Vietnam,

²Laboratory of Computational Chemistry and Modelling (LCCM), Quy Nhon University, Quy Nhon, Vietnam

* Corresponding author: Email: nguyentientrung@qnu.edu.vn

Table S1. Intermolecular parameters (r: distances in Å, θ: angles in °, q: NBO charge in e) in the binary systems formed between CH₃CHZ and RCZOH (R = CH₃, H, F; Z = O, S) at MP2/6–311++G(3df,2pd)

Complex	r(H···Z) (Å)		θ (°)		q (e)			
	O–H···Z7	C _{sp2} –H···Z2	∠O–H–Z	∠C _{sp2} –H–Z	Z2	H ^{a)}	Z7	H ^{b)}
CH ₃ O–O	1.747	2.337	179.5	130.3	-0.621	0.502	-0.546	0.139
CH ₃ S–O	1.720	2.826	170.2	128.2	-0.119	0.507	-0.544	0.128
HO–O	1.727	2.359	179.7	130.4	-0.607	0.500	-0.547	0.138
HS–O	1.706	2.837	171.5	129.1	-0.115	0.502	-0.545	0.127
FO–O	1.666	2.389	179.0	127.9	-0.615	0.510	-0.550	0.138
FS–O	1.639	2.846	172.2	127.5	-0.148	0.516	-0.547	0.131
CH ₃ O–S	2.265	2.233	177.9	146.7	-0.613	0.482	0.067	0.207
CH ₃ S–S	2.246	2.718	167.7	145.1	-0.098	0.485	0.082	0.195
HO–S	2.242	2.252	178.8	146.8	-0.598	0.478	0.070	0.205
HS–S	2.228	2.722	169.2	150.0	-0.093	0.478	0.084	0.194
FO–S	2.180	2.282	179.8	143.6	-0.607	0.486	0.079	0.205
FS–S	2.164	2.741	170.1	143.7	-0.126	0.490	0.093	0.195

^{a)}For H of –OH group of RCZOH in the complexes; ^{b)}For H of –CHZ group of CH₃CHZ in the complexes

Table S2. Selected parameters at the BCPs of intermolecular contacts at MP2/6-311++G(3df,2pd)

Complex	ρ(r _C), in au		∇ ² ρ(r _C), in au		H(r _C) ^{a)} , in au		E _{HB} ^{b)} , in kJ.mol ⁻¹		Comparison values
	O–H···Z7	C _{sp2} –H···Z2	(1)	(2)	(1)	(2)	(1)	(2)	
CH ₃ O–O	0.0405	0.0130	0.097	0.045	-0.0073	0.0012	-51.0	-11.4	2.1 ⁽¹⁾
CH ₃ S–O	0.0428	0.0102	0.100	0.027	-0.0084	0.0008	-55.0	-6.8	2.2 ⁽¹⁾
HO–O	0.0427	0.0125	0.098	0.042	-0.0084	0.0011	-54.5	-10.9	2.1 ⁽¹⁾
HS–O	0.0444	0.0099	0.101	0.027	-0.0094	0.0008	-57.7	-6.5	2.2 ⁽¹⁾
FO–O	0.0494	0.0115	0.103	0.040	-0.0124	0.0012	-66.6	-10.2	2.2 ⁽¹⁾
FS–O	0.0521	0.0096	0.105	0.027	-0.0142	0.0009	-71.8	-6.4	2.3 ⁽¹⁾
CH ₃ O–S	0.0264	0.0150	0.046	0.053	-0.0034	0.0015	-23.9	-13.5	1.7 ⁽²⁾
CH ₃ S–S	0.0276	0.0118	0.046	0.031	-0.0039	0.0008	-25.2	-8.1	1.7 ⁽²⁾
HO–S	0.0278	0.0145	0.046	0.051	-0.0040	0.0014	-25.6	-13.0	1.6 ⁽²⁾
HS–S	0.0283	0.0121	0.046	0.030	-0.0040	0.0007	-25.7	-8.1	1.7 ⁽²⁾
FO–S	0.0319	0.0133	0.045	0.048	-0.0060	0.0015	-30.5	-11.9	1.6 ⁽²⁾
FS–S	0.0330	0.0110	0.044	0.030	-0.0065	0.0009	-31.7	-7.6	1.6 ⁽²⁾

^{a)} the total electron energy density; ^{b)} individual energy of each hydrogen bond; ⁽¹⁾for O–H···Z7 and ⁽²⁾for C_{sp2}–H···Z2
E_{HB} in red for O–H···O7, E_{HB} in blue for O–H···S7, E_{HB} in yellow highlighted for C_{sp2}–H···O2 and E_{HB} in normal for C_{sp2}–H···S7

Table S3. Summary of stretching frequency changes of C–H bonds involving hydrogen bonds in the complexes

Complexes	Level of theory/Experiment	$\Delta\nu(\text{C}_{\text{sp}^3}\text{-H})$ (cm^{-1})	Ref
$\text{CH}_3\text{CHO}\cdots\text{H}_2\text{O}/\text{CH}_3\text{CHO}\cdots\text{2H}_2\text{O}$		6/-11	
$\text{CH}_2\text{FCHO}\cdots\text{H}_2\text{O}$	B3LYP/6-311++G(d,p)	10;13	1
$\text{CH}_2\text{FCHO}\cdots\text{2H}_2\text{O}$		-19;-21	
$\text{CH}_3\text{CFO}\cdots\text{H}_2\text{O}/\text{CH}_3\text{CFO}\cdots\text{2H}_2\text{O}$		-2/-23	
$\text{CH}_3\text{CHS}\cdots\text{H}_2\text{O}$	MP2/aug-cc-pVDZ	16.9	2
$\text{CH}_3\text{CHS}\cdots\text{2H}_2\text{O}$		26.7	
$\text{CH}_3\text{CHS}\cdots\text{3H}_2\text{O}$		15.6; -23.1	
$(\text{CH}_3\text{CHO})_2$	M062X/6-311++G(3df,3pd)	-16, -14, -8	3
$\text{CHX}_3\cdots\text{HNO}$ (X = F, Cl, Br)	MP2/6-311++G(d,p)	7÷41	4
$\text{F}_3\text{CH}\cdots\text{H}_2\text{O}$	Exp.	20.3; 32.3	5
Complexes	Level of theory/Experiment	$\Delta\nu(\text{C}_{\text{sp}^2}\text{-H})$ (cm^{-1})	Ref
$\text{RCHO}\cdots\text{H}_2\text{O}$ (R = H, F, CH ₃ , CH ₂ F, C ₂ H ₅)	B3LYP/6-311++G(d,p)	28 ÷ 53	6
$\text{CH}_3\text{CHO}\cdots\text{H}_2\text{O}/\text{CH}_3\text{CHO}\cdots\text{2H}_2\text{O}$	B3LYP/6-311++G(d,p)	52/93	1
$\text{CH}_2\text{FCHO}\cdots\text{H}_2\text{O}/\text{CH}_2\text{FCHO}\cdots\text{2H}_2\text{O}$		44/61	
$\text{CH}_3\text{CHS}\cdots\text{H}_2\text{O}$	MP2/aug-cc-pVDZ	24.0	2
$\text{CH}_3\text{CHS}\cdots\text{2H}_2\text{O}$		33.1	
$\text{CH}_3\text{CHS}\cdots\text{3H}_2\text{O}$		62.2	
$\text{XCHO}\cdots\text{H}_2\text{Z}$	MP2/aug-cc-pVDZ	2.9 ÷ 52	7
$\text{XCHO}\cdots\text{2H}_2\text{O}$ (X = H, F, Cl, Br, CH ₃ ; Z = O, S)		4.0 ÷ 92.3	
$\text{RCHZ}\cdots\text{HCOOH}$ (R = H, F, Cl, Br, CH ₃ , NH ₂ ; Z = O, S)	MP2/aug-cc-pVDZ	81÷96	8
$\text{RCHO}\cdots\text{R}'\text{OH}$ (R = NH ₂ , CF ₃ , CH ₃ O, CN, H; R' = H, CH ₃ , NH ₂ , C(O)H)	MP2/cc-pVTZ	23.01 ÷ 92.69	9
$(\text{CH}_3\text{CHO})_2$	M062X/6-311++G(3df,3pd)	50	3
	MP2/6-311++G(d,p)	-	10
	MP2/6-31+G(d)	56.3; 56.6	11
$\text{HCHO-NH}_2\text{OH}$	Exp.	14.6	12
$\text{CH}_3\text{COCHO-NH}_2\text{OH}$		16.3	
$\text{CHOCHO}\cdots\text{H}_2\text{O}_2$	Exp.	28.9	13
$\text{CHOCHO}\cdots\text{H}_2\text{O}$	Exp.	2.5	14
$\text{CHOCHO}\cdots\text{H}_2\text{O}$	Exp.	14.7	14
4-fluorobenzaldehyde dimer	Exp.	8	15
2-methoxybenzaldehyde dimer	Exp.	21	16
Complexes	Level of theory	$\Delta\nu(\text{C}_{\text{sp}}\text{-H})$ (cm^{-1})	Ref
$\text{C}_2\text{HX}\cdots\text{C}_6\text{H}_6$ (X = H, F, Cl, Br, CH ₃ , NH ₂)	MP2/aug-cc-pVDZ	-15.7 ÷ -24.9	17
$\text{C}_2\text{H}_2\cdots\text{C}_2\text{H}_2$	MP2/aug-cc-pVTZ	-21	18
$\text{C}_2\text{H}_2\cdots\text{HCN}$		-61	
$\text{C}_6\text{H}_6\cdots\text{C}_2\text{H}_2$		-17	
$\text{C}_6\text{H}_6\cdots\text{HCN}$		-50	

1. A. K. Chandra and T. Zeegers-Huyskens, *J. At. Mol. Opt. Phys.*, 2012, **2012**, e754879.
2. N. T. T. Cuc, H. Q. Dai, N. T. A. Nhung, N. P. Hung and N. T. Trung, *Vietnam J. Chem.*, 2019, **57**, 425–432.
3. T. S. Thakur, M. T. Kirchner, D. Bläser, R. Boese and G. R. Desiraju, *Phys. Chem. Chem. Phys.*, 2011, **13**, 14076–14091.
4. N. T. Trung, T. T. Hue and M. T. Nguyen, *Phys. Chem. Chem. Phys.*, 2009, **11**, 926–933.
5. C. D. Keefe and M. Isenor, *J. Phys. Chem. A*, 2008, **112**, 3127–3132.
6. A. K. Chandra and T. Zeegers-Huyskens, *J. Comput. Chem.*, 2012, **33**, 1131–1141.
7. N. T. T. Cuc, C.-T. D. Phan, N. T. A. Nhung, M. T. Nguyen, N. T. Trung and V. T. Ngan, *J. Phys. Chem. A*, 2021, **125**, 10291–10302.
8. N. T. Trung, P. N. Khanh, A. J. P. Carvalho and M. T. Nguyen, *J. Comput. Chem.*, 2019, **40**, 1387–1400.
9. D. Kaur and R. Kaur, *J. Chem. Sci.*, 2015, **127**, 1299–1313.
10. A. Kovács, A. Szabó, D. Nemesok and I. Hargittai, *J. Phys. Chem. A*, 2002, **106**, 5671–5678.
11. Y. Yang and W. Zhang, *Acta Chim. Sin.*, 2009, **67**, 599–606.
12. B. Golec, M. Sałdyka and Z. Mielke, *Mol. Basel Switz.*, 2021, **26**, 1144.
13. M. Mucha and Z. Mielke, *Chem. Phys. Lett.*, 2009, **482**, 87–92.
14. M. Mucha and Z. Mielke, *J. Phys. Chem. A*, 2007, **111**, 2398–2406.
15. P. J. A. Ribeiro-Claro, M. P. M. Marques and A. M. Amado, *ChemPhysChem*, 2002, **3**, 599–606.
16. P. J. A. Ribeiro-Claro, M. G. B. Drew and V. Félix, *Chem. Phys. Lett.*, 2002, **356**, 318–324.
17. P. Khanh, V. Ngan, N. Man, N. T. Ai Nhung, A. Chandra and N. Trung, *RSC Adv.*, 2016, **6**, 106662–106670.
18. P. Jantimapornkij, P. Jundee, N. Uttamapinant, S. Pianwanit and A. Karpfen, *Comput. Theor. Chem.*, 2012, **999**, 231–238.

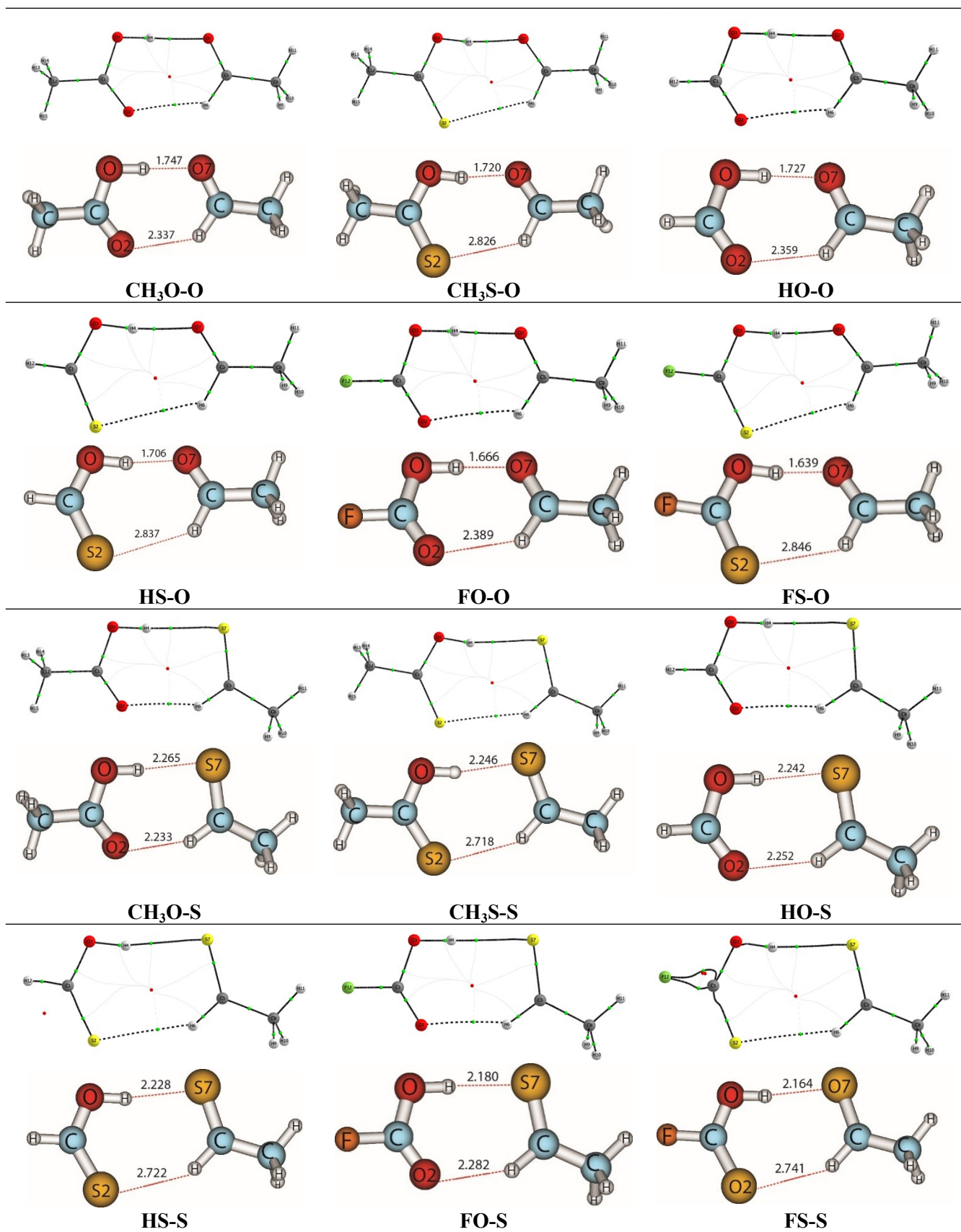


Figure. S1. Topological geometries and stable structures of complexes plotted at MP2/6-311++G(3df,2pd) (values of distance in Å)

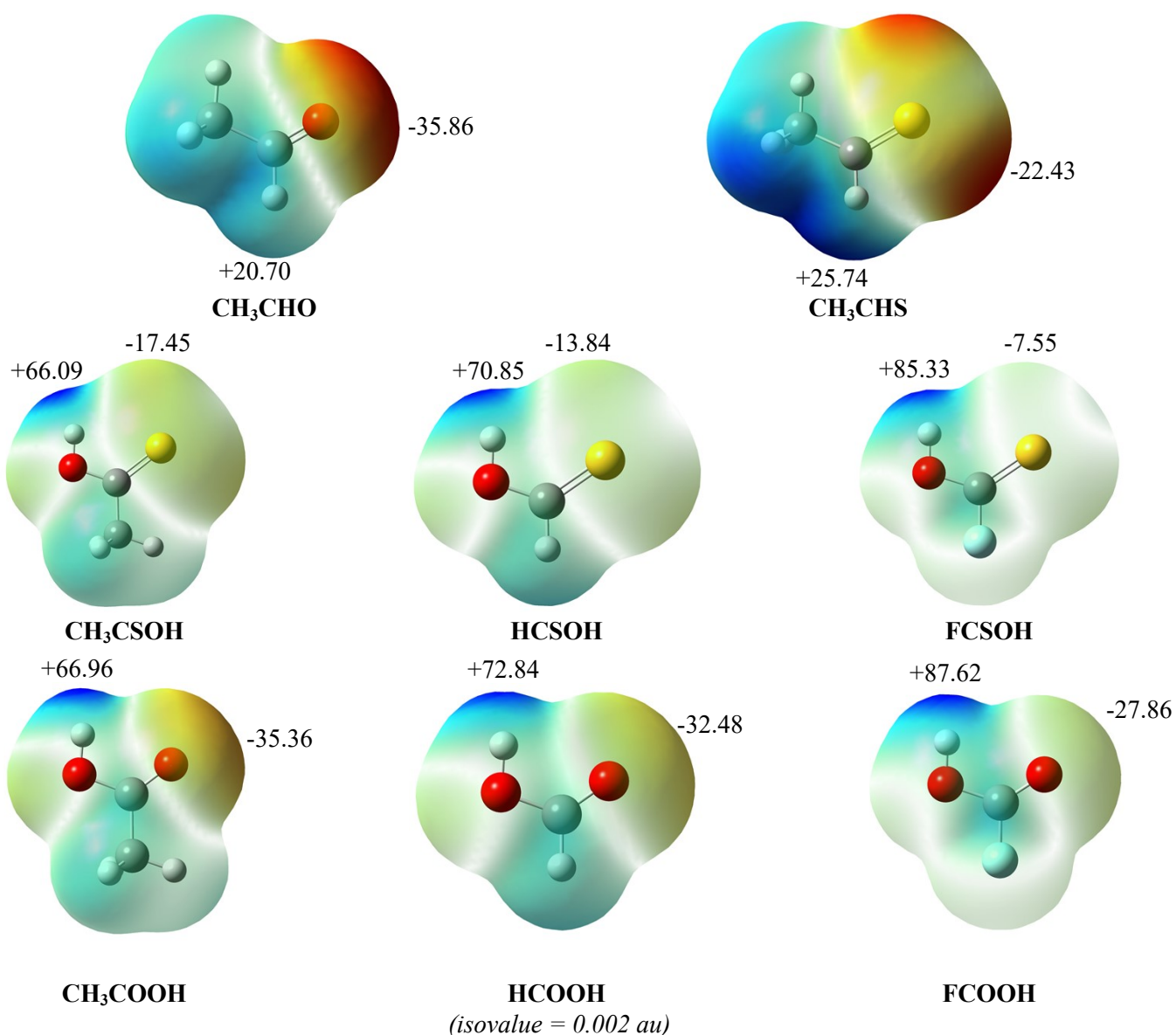


Figure. S2. Molecular electrostatic potential (in kcal.mol^{-1}) of the CH_3CHZ and RCZOH ($\text{R} = \text{CH}_3, \text{H}, \text{F}; \text{Z} = \text{O}, \text{S}$) at MP2/6-311++G(3df,2pd) level

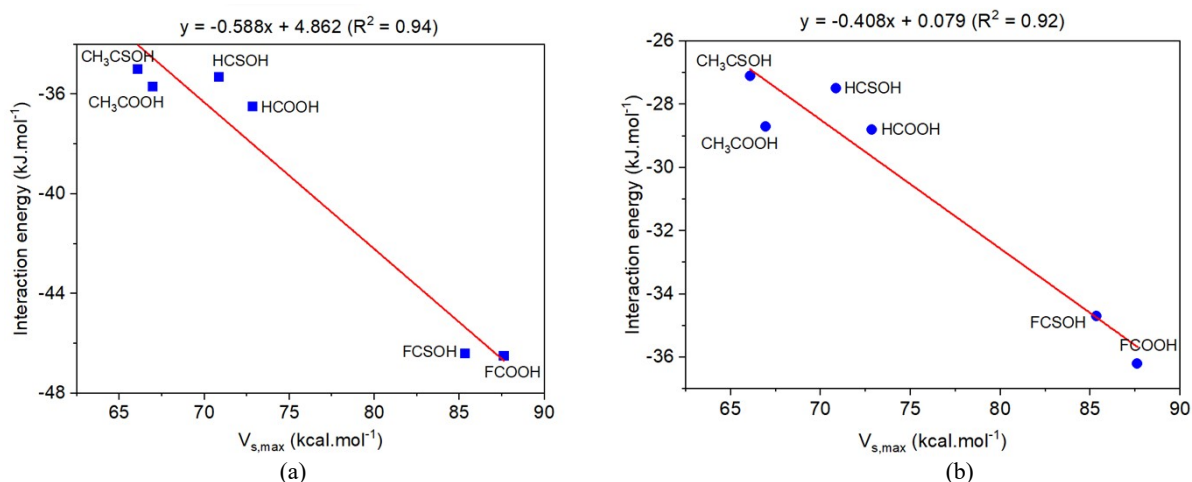


Figure. S3. Relationship of the interaction energies of the investigated complexes for CH_3CHO -complexes (a) and for CH_3CHS -complexes (b) with electrostatic potential of H atom in monomers acting as proton donor at MP2/6-311++G(3df,2pd) level.

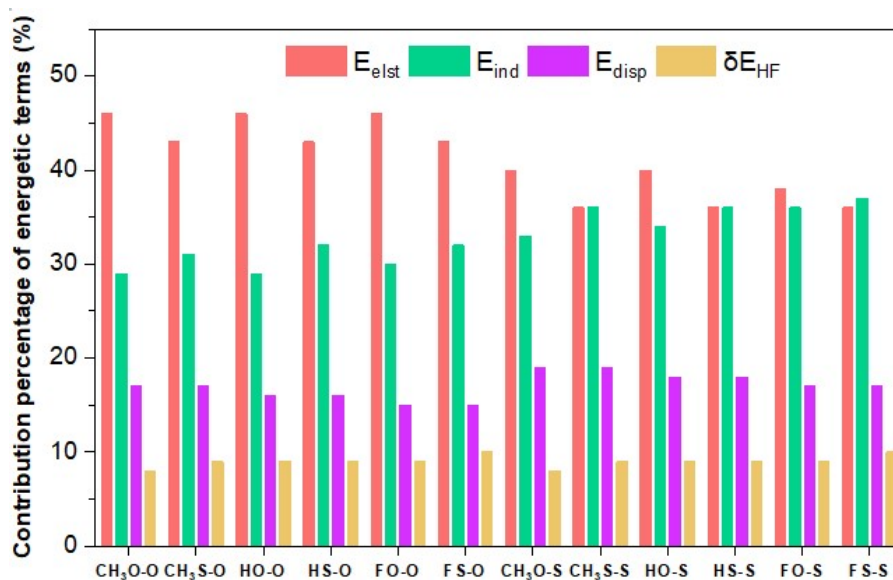


Figure. S4. Diagram for contribution percentage of different energy components into total stabilization energy of the complexes for $RCZOH \cdots CH_3CHZ$, with $R = CH_3, H, F$; $Z = O, S$

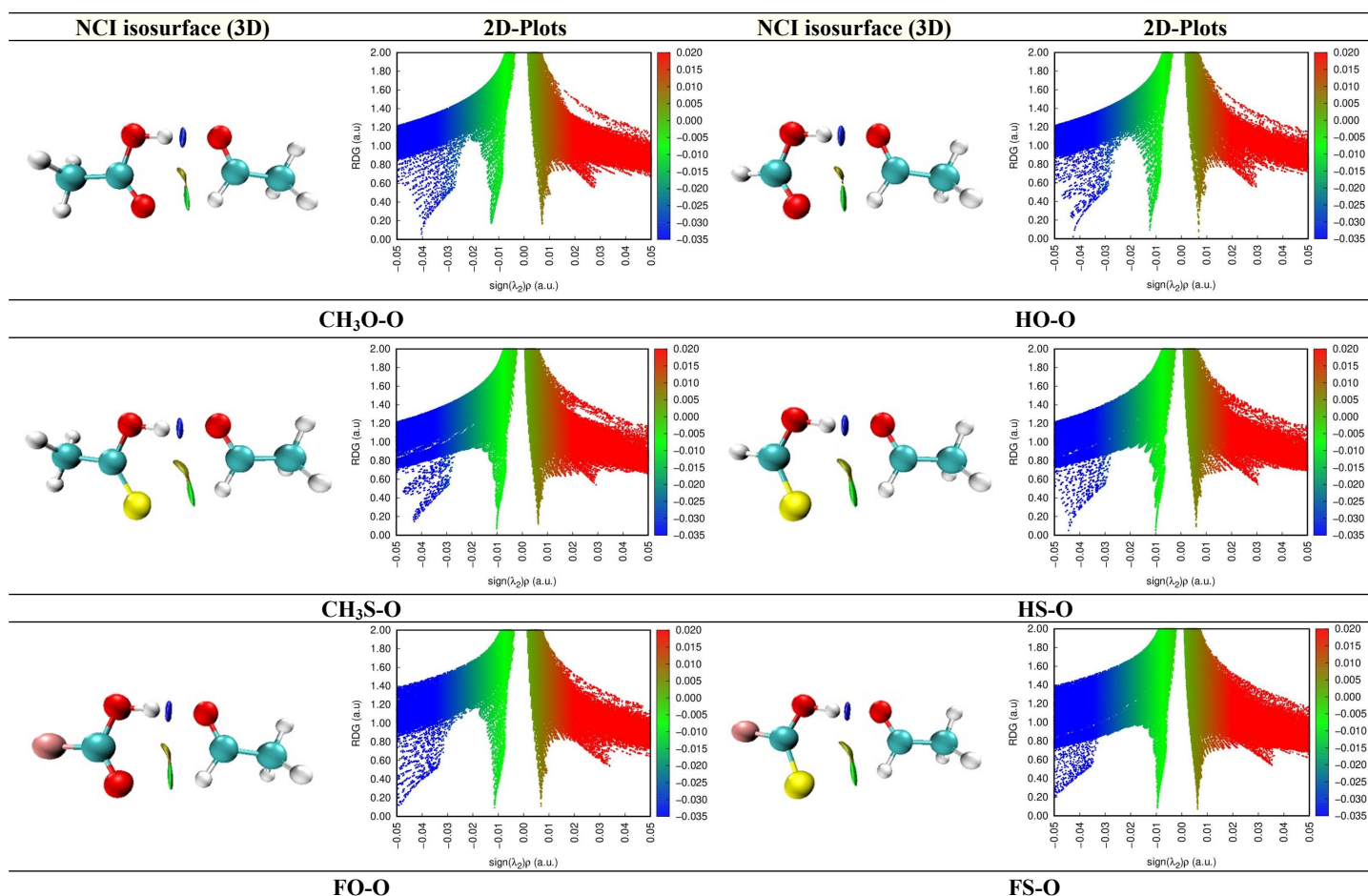


Figure. S5a. NCI isosurface and 2D-plots of reduced density gradient (RDG) versus the electron density multiplied by the sign of the second Hessian eigenvalue ($sign(\lambda_2)\rho(r_C)$) for $RZ-O$ complexes, with $R = CH_3, H, F$; and $Z = O, S$.
(The surfaces are colored on a blue-green-red scale according to the values of $sign(\lambda_2)\rho(r_C)$ ranging from -0.05 to 0.05 au)

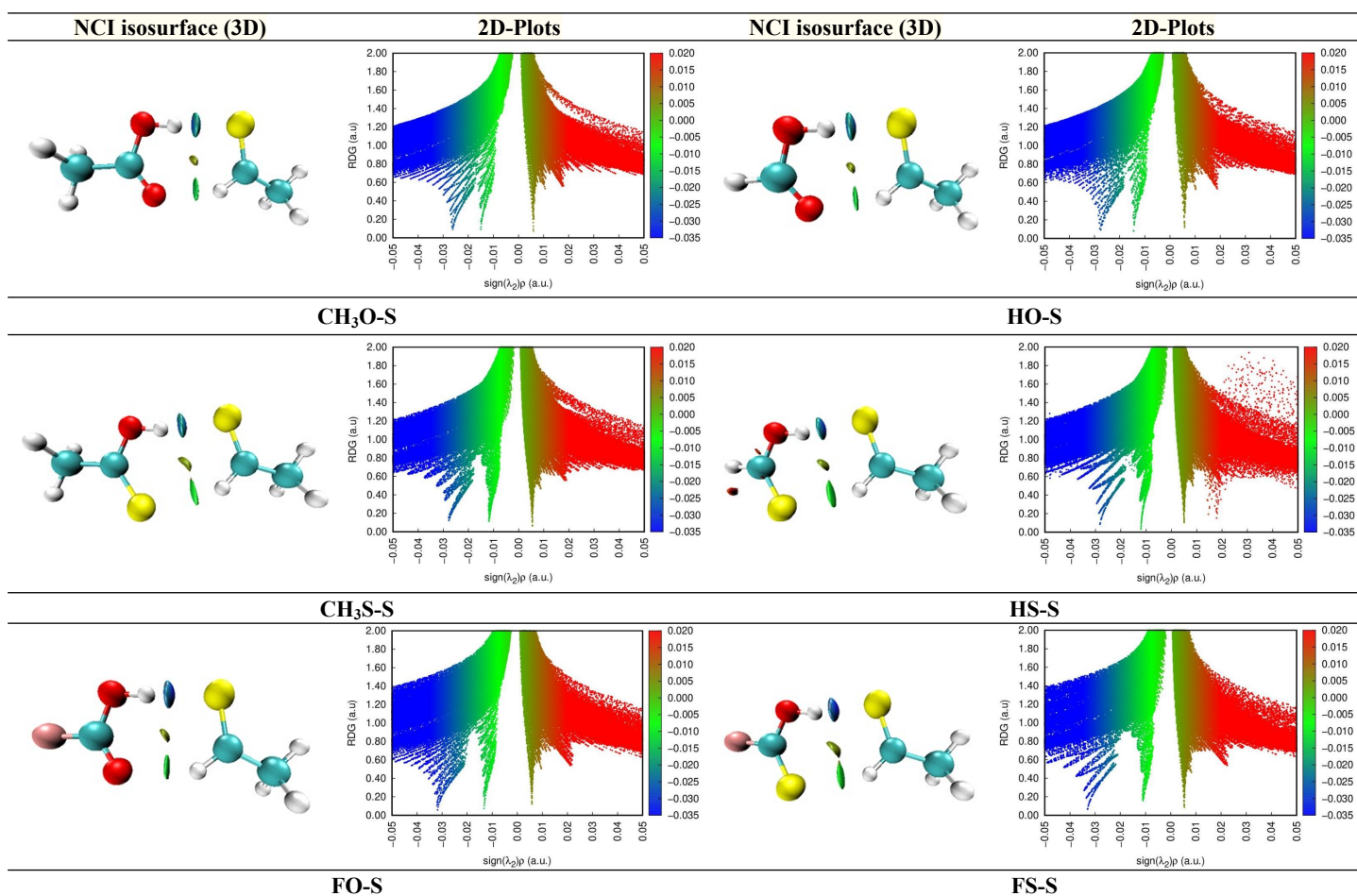


Figure. S5b. NCI isosurface and 2D-plots of reduced density gradient (RDG) versus the electron density multiplied by the sign of the second Hessian eigenvalue ($\text{sign}(\lambda_2)\rho(r_c)$) for **RZ-S** complexes, with R= CH₃, H, F; and Z = O, S
(The surfaces are colored on a blue-green-red scale according to the values of $\text{sign}(\lambda_2)\rho(r_c)$ ranging from -0.05 to 0.05 au)

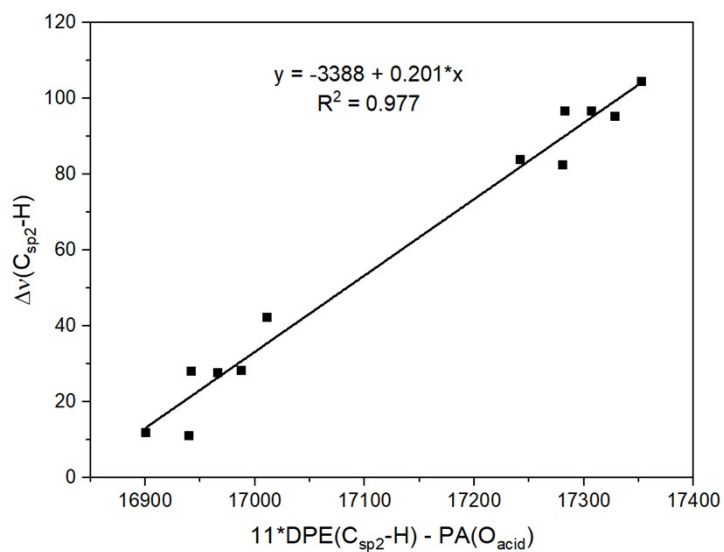


Figure. S6. The linear correlation of $\Delta\nu(\text{C}_{\text{sp}^2}\text{-H})$ (in cm^{-1}) versus $\text{DPE}(\text{C}_{\text{sp}^2}\text{-H})$ (in $\text{kJ}\cdot\text{mol}^{-1}$) of CH₃CHZ and PA(O) (in $\text{kJ}\cdot\text{mol}^{-1}$) of RCZOH

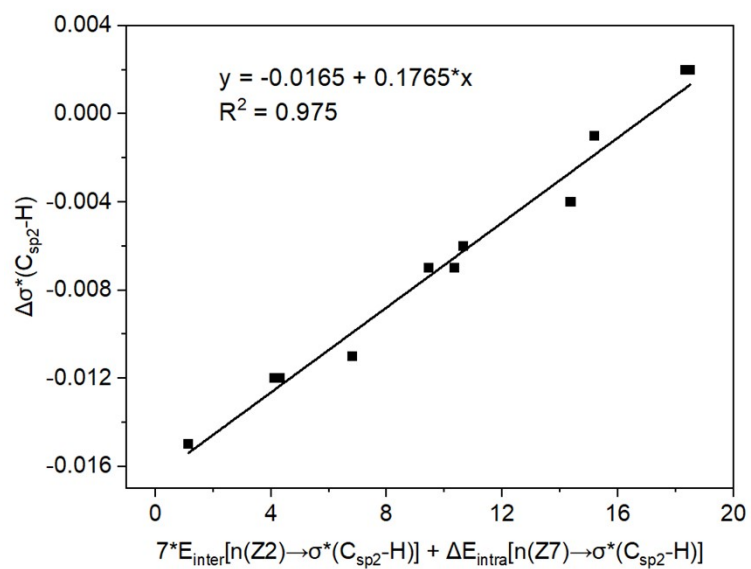


Figure. S7. The linear correlation of $\Delta\sigma^*(C_{sp^2}-H)$ (in electron) versus intermolecular hyperconjugative interaction energies (in kJ.mol⁻¹) and changes of intramolecular hyperconjugative interaction energies ($7*E_{inter} + \Delta E_{intra}$) (in kJ.mol⁻¹) for the complexes